Protons and light fragments in Ar+KCl at 1.76 AGeV measured with HADES

Heidi Schuldes[1], Manuel Lorenz[1,2] (for the HADES-Collaboration)
[1]Goethe-University Frankfurt, [2]Utrecht University
E-mail: h.schuldes@gsi.de

Abstract. We present transverse momentum spectra, rapidity distributions and multiplicities of protons, deuterons and tritons measured with the High Acceptance DiElectron Spectrometer HADES in the reaction Ar(1.76A GeV)+KCl. This completes the HADES data set measured in this reaction, comprising dielectrons and various lighter hadrons.

1. Introduction

The investigation of rare and penetrating probes in heavy-ion collisions (HIC) has attracted much interest in the recent years over all accessible collision energies. The ultimate hope is to find key observables sensitive to the onset of deconfinement [1, 2, 3], the critical point [4, 5] and chiral symmetry restoration [6, 7]. In practice it turned out that in order to extract quantitative and most of the time also qualitative results the observed production rates or phase-space distributions have to be compared to phenomenological models. To do so these models have to describe the global event characteristics first. Unfortunately, data on these global characteristics like rapidity distributions and transverse momentum spectra of e.g. protons can be rare at some energies/systems. At SIS energies valuable systematics have been collected and published by the FOPI collaboration in [8] mostly for central Au+Au collisions. Although this data covers the same energy range and include some variations of the size of the collision system, the extrapolation to semi-central collisions of Ar+KCl measured by HADES at a kinetic beam energy of 1.76 AGeV exhibit large uncertainties. Recently, the HADES collaboration had a Au+Au beamtime at 1.23 AGeV incident kinetic energy. To understand the data from the heavier system, it is important to investigate as many observables as possible in the lighter systems.
Apart from the dielectron yield [9] HADES has published hadron yields from the Ar+KCl data for this energy regime [9]. The aim of this paper is to complete the published data set by adding transverse momentum spectra, rapidity distributions and multiplicities of protons, deuterons and tritons.

2. Experiment and Analysis

HADES is a charged-particle detector consisting of a 6-coil toroidal magnet centered on the beam axis and six identical detection sections located between the coils. A detailed description of HADES is given in [10]. For the presented data an Argon beam of $\sim 10^6$ particles/s was incident with a beam energy of 1.76 AGeV on a four-fold segmented KCl target with a total

thickness corresponding to 3.3 % interaction probability. A fast diamond start detector located upstream of the target was intercepting the beam and was used to determine the time-zero information. The data readout was started by a first-level trigger (LVL1) requiring a charged-particle multiplicity ≥ 16, in the TOF/TOFino detectors. Based on a full GEANT simulation, employing realistic detector responses of Ar+KCl events generated with the UrQMD transport model [11], we found that the event ensemble selected by this (LVL1) trigger condition has a mean number of participating nucleons ($\langle A_{part} \rangle$) equal to 38.5 ± 3.9.

The particle identification was done by a velocity vs. momentum $\times$ polarity correlation, where the velocity was determined by the time-of-flight measurement in the TOF and TOFino scintillators with respect to the time-zero information and the tracked flight path. If needed, additional particle discrimination power was gained from the energy loss (dE/dx) information in the MDC and scintillators. This is illustrated in Fig. 1 where the mass distribution in the TOF-region is plotted after application of track quality selections (dark blue) and after an additional selection on e.g. deuterons making use of the energy loss information (light blue).

The yields of the different particles are assessed as a function of rapidity y and transverse

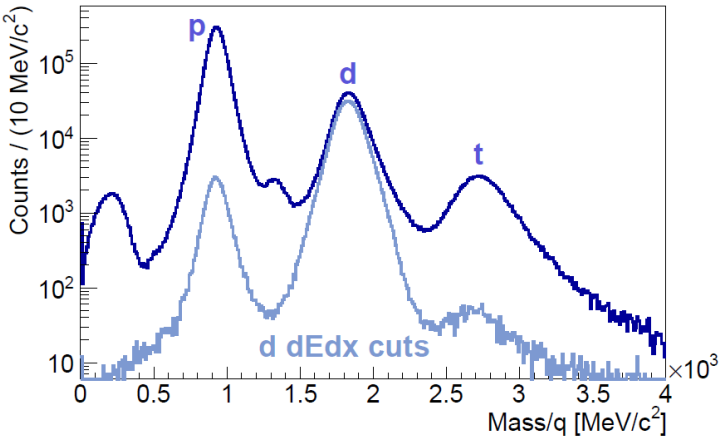

Figure 1: Mass distribution in the TOF-region after application of track quality selections (dark blue) and after additional selection on deuterons making use of the energy loss information (light blue).

mass $m_t - m_0$. Efficiency and acceptance losses are corrected for a given y and $m_t - m_0$ region iteratively using simulated data embedded into real events. In a first step the momentum distribution of the simulated particles was assumed with a white distribution, while finally with a distribution very similar to the experimentally observed assuming a thermal source of a temperature T=80 MeV and a constant radial expansion velocity β_r of 0.4. We find however only little sensitivity of the input on the correction factor (at the order of 1% in the overall correction per given region). The combined correction factor for losses due to efficiency and acceptance as a function of $m_t - m_0$ for the y region $0.4 \leq$ y ≤ 0.45 is displayed in Fig. 2 separately for p, d and t. For further details on particle identification and the data analysis of charged hadrons we refer to [12, 13, 14].

3. Phase-space Distributions

The resulting transverse mass spectra are displayed in Fig. 4. In order to extrapolate to the unmeasured regions the spectra are described using the following function according to Siemens-Rasmussen:

$$\frac{dN}{2\pi m_t dm_t dy} = c \cdot E \cdot \exp\left(-\frac{\gamma \cdot E}{T}\right) \cdot \frac{\sinh \alpha}{\alpha} - \frac{T}{E} \cdot \cosh \alpha, \qquad (1)$$

with $\alpha = (\gamma \cdot \beta_r \cdot p)/T$ and $\gamma = 1/\sqrt{1-\beta_r^2}$. T, β_r and the constant C are free parameters. T can be associated with the temperature of a thermal source and β_r with its radial expansion

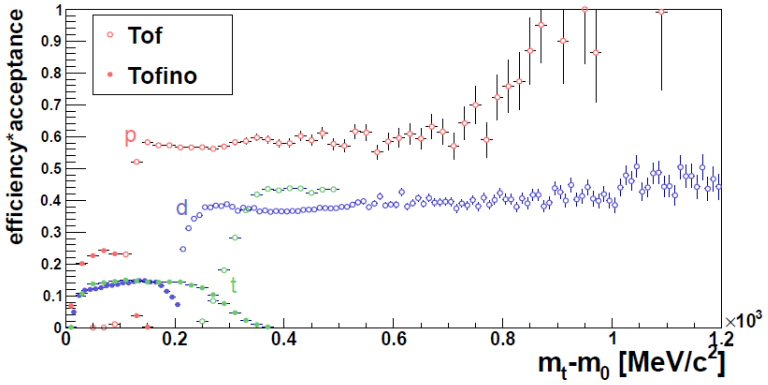

Figure 2: Combined correction factor for losses due to efficiency and acceptance as a function of $m_t - m_0$ for $0.4 < y < 0.45$ for both Tof-systems TOFino and TOF and the different particles p, d and t.

velocity. In this picture T and β_r should not depend on y. Hence a χ^2 scan in the $T - \beta_r$-plane is done globally for all three particles. The χ^2/dof distribution for the global scan is displayed in Fig. 3. As the values of χ^2/dof indicate, some spectra cannot be reproduced based on the scenario of a radially flowing thermal source.
To obtain rapidity distributions we integrate the measured data points and use the parameters of the global scan (the corresponding Siemens-Rasmussen fits are displayed together with the spectra in Fig. 4) in order to extrapolate down to small m_t and up to infinity. The resulting yields as a function of y are displayed in Fig. 5, together with the yields from integrating the distribution within the measured limits. This allows to judge on the systematic error introduced by the extrapolation down to small transverse mass.

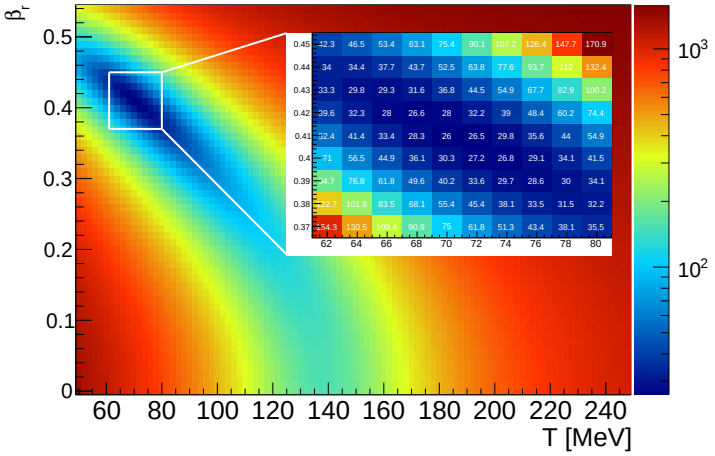

Figure 3: χ^2/dof distribution in the $T-\beta_r$-plane from fitting p, d and t transverse mass spectra simultaneously with Eq. 1 (see text).

4. Discussion and Conclusion

In semi-central Ar+KCl collisions at 1.76 AGeV incident kinetic energy, the rapidity distributions of p, d and t exhibit distinct local maxima close to target/projectile rapidity. The location of the maximum differential count rate dN/dy moves closer to target/projectile rapidity, respectively, the heavier the mass of the particle is, e.g. comparing protons with tritons. Also, heavier particles are more abundant close to target/projectile rapidity than at midrapidity.

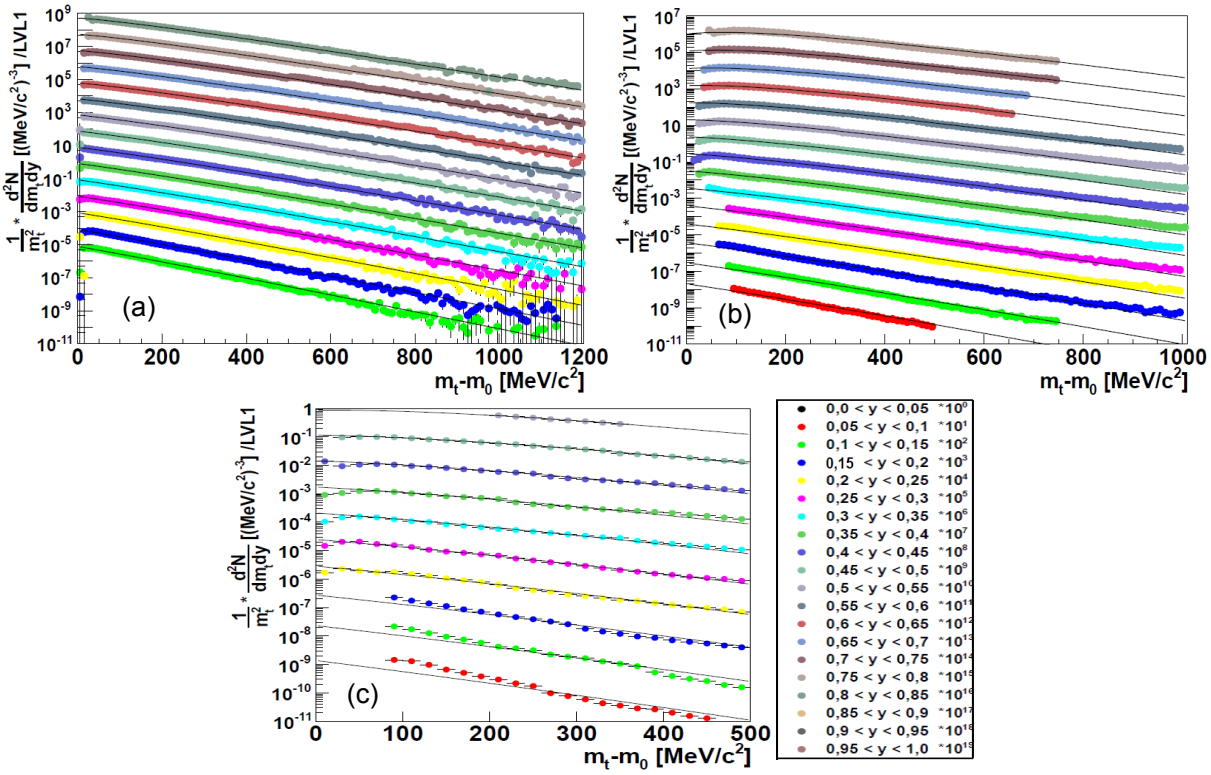

Figure 4: Efficiency and acceptance corrected transverse mass spectra of protons (a) (rapidity range $0.1 \leq y \leq 1$), deuterons (b) (rapidity range $0.05 \leq y \leq 0.8$) and tritons (c) (rapidity range $0.05 \leq y \leq 0.55$) scaled with exponentials. Black lines correspond to Siemens-Rasmussen-functions with fixed parameters for temperature and radial flow (see text).

This experimental observation is consistent with a scenario, where heavier particles do mainly origin from target/projectile fragmentation in this reaction system. However, the position of the two peaks are slightly shifted away from target/projectile rapidity which might be explained by a convolution of a thermal like source sitting at midrapidity and sources at target/projectile rapidity. In addition, this effect might be enhanced due to the low p_t-acceptance-cutoff acting stronger on the target/projectile-source then on the thermal one. It is interesting to note that indeed, the spectral distribution can be simultaneously parametrized assuming a thermal source at midrapidity with T=70±7 MeV, which radially expands with β_r=0.41±0.03. these numbers are compatible with results from other analyses in the SIS18 energy range and emphasize the role of (radial) flow on the emission of particles in this energy regime.

The analysis, together with the broad set of published particle yields demonstrate the outstanding particle identification capabilities of the HADES detector, even for heavy fragments. After a detector upgrade, where for example the TOFino szintillator wall was replaced by a resistive plate chamber and a forward wall was installed, the collaboration recorded 7.3 x 10^9 events of Au+Au collisions at 1.23 AGeV. With this improved setup refined data of particle production at SIS18 energies, covering fragment emission as well, will be soon available [15, 16].

We gratefully acknowledge the HADES-Collaboration, GSI, HIC for FAIR and HGS-HIRe.

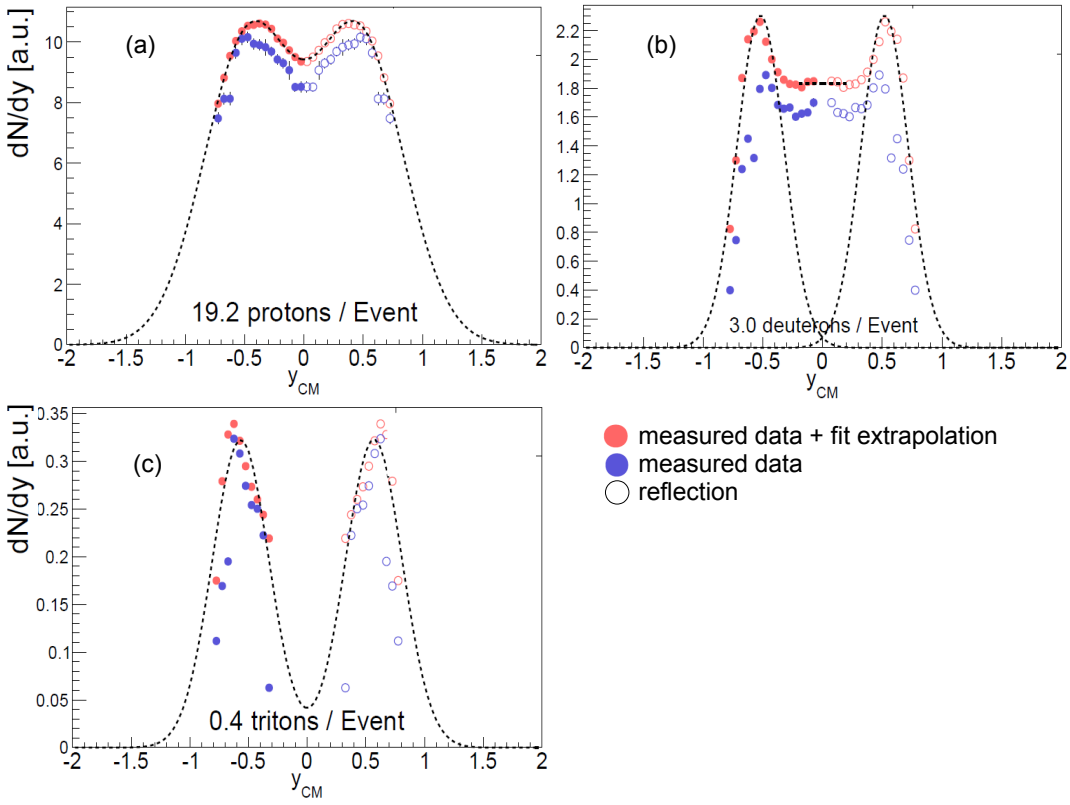

Figure 5: dN/dy-distribution of protons (a), deuterons (b) and tritons (c) from integrating the distribution within the measured limits (blue) and extrapolated with Siemens-Rasmussen-functions (red). Dashed lines correspond to two gaussian (plus polynomial for d) parametrizations to estimate the total yield of the particles.

References

[1] E.V.Shuryak, Phys.Lett.B**78** (1978) 150 [Sov.J.Nucl.Phys.**28** (1978) 408] [Yad.Fiz.**28** (1978) 796].

[2] T. Matsui and H. Satz, Phys. Lett. B **178** (1986) 416.

[3] J. Rafelski and B. Muller, Phys. Rev. Lett. **48** (1982) 1066 [Erratum-ibid. **56** (1986) 2334].

[4] Z. Fodor and S. D. Katz, JHEP **0404** (2004) 050 [hep-lat/0402006].

[5] M. A. Stephanov, K. Rajagopal and E. V. Shuryak, Phys. Rev. D **60** (1999) 114028 [hep-ph/9903292].

[6] S. Weinberg, Phys. Rev. **166** (1968) 1568.

[7] R. Rapp and J. Wambach, Adv. Nucl. Phys. **25** (2000) 1 [hep-ph/9909229].

[8] W. Reisdorf *et al.* (FOPI Collaboration), Nucl. Phys. A **876** 1 (2012).

[9] G. Agakishiev *et al.* (HADES Collaboration), Phys. Rev. C **84**, 014902 (2011); Phys. Rev. C **80**, 025209 (2009); Phys. Rev. C **82**, 044907 (2010); Phys. Rev. Lett. **103**, 132301 (2009); Eur. Phys. J. A **47** 21 (2011).

[10] G. Agakishiev *et al.* (HADES Collaboration), Eur. Phys. J. A **41**, 243 (2009).

[11] S. A. Bass *et al.*, Prog. Part. Nucl. Phys. **41** 225 (1998).

[12] A. Schmah, PhD thesis, Technical University Darmstadt, Darmstadt (2008).

[13] M. Lorenz, PhD thesis, Goethe-Universität, Frankfurt (2012).

[14] H. Schuldes, Master thesis, Goethe-Universität, Frankfurt (2012).

[15] M. Lorenz (HADES Collaboration), NUPHA 20167 (2014).

[16] T. Galatyuk (HADES Collaboration), NUPHA 20289 (2014).